

Two-dimensional adatom gas phase on the Si(111)- $\sqrt{3} \times \sqrt{3}$ -Ag surface directly observed by scanning tunneling microscopy

Norio Sato

Department of Physics, Graduate School of Science, University of Tokyo, 7-3-1 Hongo, Bunkyo-ku, Tokyo 113-0033, Japan

Tadaaki Nagao

Department of Physics, Graduate School of Science, University of Tokyo, 7-3-1 Hongo, Bunkyo-ku, Tokyo 113-0033, Japan and Core Research for Evolutional Science and Technology, The Japan Science and Technology Corporation, Kawaguchi Center Building, Hon-cho 4-1-8, Kawaguchi, Saitama 332-0012, Japan

Shuji Hasegawa*

Department of Physics, Graduate School of Science, University of Tokyo, 7-3-1 Hongo, Bunkyo-ku, Tokyo 113-0033, Japan and Core Research for Evolutional Science and Technology, The Japan Science and Technology Corporation, Kawaguchi Center Building, Hon-cho 4-1-8, Kawaguchi, Saitama 332-0012, Japan

(Received 25 June 1999)

Excess Ag adatoms of submonolayer coverages on top of the Si(111)- $\sqrt{3} \times \sqrt{3}$ -Ag surface at room temperature (RT) are known to stay in a two-dimensional adatom-gas (2DAG) phase as a thermodynamical equilibrium state. Reducing the diffusion mobility of the Ag adatoms by cooling the substrate down to 62 K, we could observe migrating adatoms in the 2DAG phase directly by scanning tunneling microscopy (STM). The individual Ag adatoms ceased migration completely at 6 K, showing starlike patterns in STM images. The estimated amount of those Ag adatoms frozen at 6 K was on the order of 0.01 ML, which is in accordance with that at RT obtained previously from electrical conductance measurements. [S0163-1829(99)14847-1]

I. INTRODUCTION

Thermal adatoms, here called ‘‘two-dimensional adatom gas (2DAG),’’ are mobile atoms adsorbed on surfaces equilibrated with ‘‘reservoirs’’ such as their two (2D) or three-dimensional (3D) nuclei or step edges on surfaces, much like a 3D vapor in equilibrium with its condensed substance.¹ Surface diffusion of such a 2DAG plays crucial roles in a variety of surface dynamical phenomena such as epitaxial growth, Ostwald ripening, electromigration, thermal desorption, and surface phase transitions between phases having different atom densities.

Also on the Si(111)- $\sqrt{3} \times \sqrt{3}$ -Ag surface, the 2DAG phase is already seen to explain the zeroth-order thermal desorption of Ag atoms from this surface,^{2,3} electromigration phenomena,⁴ and a change in photoemission spectra.^{5,6} From the electrical conductance measurements on this surface at room temperature (RT), it has been found that additionally deposited Ag atoms on top of the $\sqrt{3} \times \sqrt{3}$ -Ag surface makes a supersaturated metastable 2DAG phase when the additional Ag coverage is less than ~ 0.03 ML.⁷ Ag atoms in the 2DAG phase donated their valence electrons into a surface-state band of the substrate, resulting in an increase of electrical conductance.⁸ Such a gas phase in a supersaturated metastable state has also been shown by theoretical simulations.⁹ But it is almost impossible to directly observe the 2DAG at RT even with an atomic resolution probe such as scanning tunneling microscopy (STM), because the individual Ag adatoms in the 2DAG phase migrate with very high speed, far beyond the time resolution in STM imaging.

However, in the present work we have succeeded in ob-

serving the 2DAG phase directly using low-temperature STM. As the temperature of the substrate is decreased from RT, the mobility of the Ag adatoms forming the 2DAG phase becomes reduced, and at last, they cease migrating at enough low temperatures. By controlling the temperature and the coverage of the Ag adatoms on top of the $\sqrt{3} \times \sqrt{3}$ -Ag surface, migrating Ag adatoms actually became observable at 62 K. At 6 K, the Ag adatoms are at rest equally spaced from each other, showing characteristic starlike patterns. From the images at 6 K, the amount of Ag adatoms having formed the 2DAG phase was estimated to be of the order of 0.01ML. This is in accordance with the critical coverage of the 2DAG phase, 0.03ML, estimated in the previous measurements of the surface electrical conductance.^{7,8}

II. EXPERIMENT

We used a commercial ultrahigh-vacuum low-temperature STM (UNISOKU USM501 type), combined with reflection high-energy electron diffraction (RHEED) system for preparing sample surfaces. The base pressure in the chambers was less than 1×10^{-10} Torr. The sample can be cooled down to 62 K with supercooled liquid nitrogen, or 6 K with liquid helium at the STM stage attached to those liquid containers. The temperature of the Si wafer was monitored with an AuFe-chromel thermocouple attached near the sample. The substrate was an *n*-type Si(111) wafer with 0.005 Ω cm resistivity at RT. We used an electrochemically etched polycrystalline tungsten tip followed by *in situ* electron bombardment cleaning.

After making the clean 7×7 surface by flashing at

1200 °C several times, the $\sqrt{3}\times\sqrt{3}$ -Ag surface was prepared by depositing just 1 ML or more than 1 ML of Ag at 500 °C. Precise coverage controls were done by *in situ* RHEED observations during the Ag deposition with a constant rate. The saturation coverage of the $\sqrt{3}\times\sqrt{3}$ -Ag surface is 1 ML.^{10,11} After the completion of the $\sqrt{3}\times\sqrt{3}$ -Ag surface, the sample was cooled down to RT in 1 h, and, then, transferred to the STM stage which had been already cooled down to low temperatures. All the samples were cooled down in this way, and waited for 2–3 h until the temperature of the sample became equilibrated with that of the STM stage. The additional Ag atoms were sometimes deposited at the cold STM stage, and then we began STM observations. We chose several ways for sample preparation to reveal the properties of the 2DAG phase. Though they will be described in detail at each stage in the following, important points in sample preparation are (1) amounts of Ag deposited at 500 °C (just 1 ML or more than 1 ML) at preparing the $\sqrt{3}\times\sqrt{3}$ -Ag structure; (2) amounts of Ag additionally deposited at low temperatures (zero or sub-monolayers) on top of the $\sqrt{3}\times\sqrt{3}$ -Ag surface, and (3) annealing temperatures after the additional Ag deposition at low temperature.

III. RESULTS AND DISCUSSIONS

A. Frozen 2DAG

The surface in Figs. 1(a) and 1(b) was prepared in the following way. After 1.7 ML of Ag was deposited on the 7×7 clean surface at 500 °C to obtain the $\sqrt{3}\times\sqrt{3}$ RHEED pattern, the sample was kept at RT for 1 h then transferred to the STM stage at 6 K. We performed STM observations *without* additional Ag deposition at 6 K. The sample bias voltage of the image was 1.4 V with respect to the tip, probing the sample empty states. Since the saturation Ag coverage of the $\sqrt{3}\times\sqrt{3}$ -Ag structure is 1.0 ML, the majority of the excess Ag (0.7 ML) makes 3D Ag islands such as seen in the center of Fig. 1(b) or much larger islands (Stranski-Krastanov mode), but there are a small percentage of the excess Ag atoms forming the 2DAG seen as random bright stars in Fig. 1. The surface in Fig. 1(c) was prepared by the similar procedures as for Figs. 1(a) and 1(b), but with a Ag coverage of 1.2 ML.

There can be seen two types of isolated adsorbates with threefold symmetry on the terrace of the $\sqrt{3}\times\sqrt{3}$ -Ag surface in Fig. 1(a): smaller adsorbates indicated by A and larger adsorbates indicated by B. Magnified images of these adsorbates are shown in Fig. 2. Here the smaller adsorbates indicated by A are called ‘‘Ag stars,’’ and the larger adsorbates indicated by B ‘‘Ag propellers.’’ Since an Ag star is the smallest unit observed in a lot of images, it is most likely that the Ag star is a single Ag adatom, while the Ag propeller consists of several, probably three, Ag adatoms.

Based on a recently proposed asymmetric structure, called the inequivalent triangle (IET) model, for the $\sqrt{3}\times\sqrt{3}$ -Ag surface at low temperatures,^{12,13} the surface shows a hexagonal-lattice pattern in an empty-state STM image at low temperature [Figs. 1 and 2(a)–2(c)], in contrast to a honeycomb pattern at room temperature.¹⁴ Two Ag triangles in the $\sqrt{3}\times\sqrt{3}$ unit cell are different in size, resulting in an asymmetric distribution in the local density of states in the

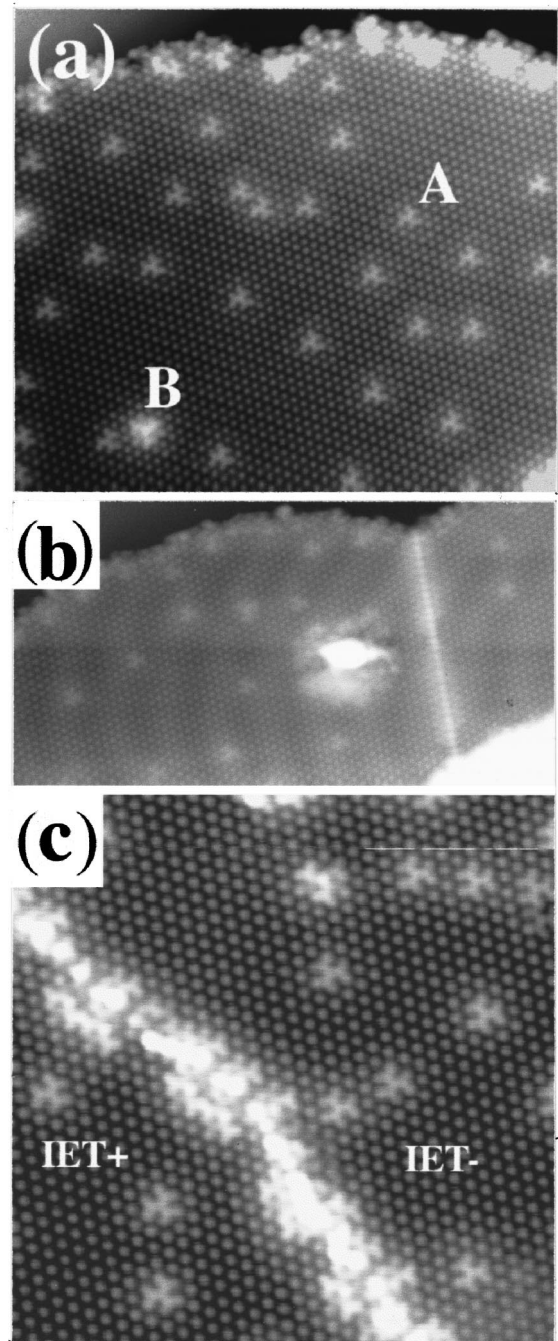


FIG. 1. (a) An empty-state STM image ($325\times 380\text{ \AA}^2$) with a sample bias voltage $V=1.4\text{ V}$, and tunneling current $I=0.5\text{ nA}$ taken in the constant-current mode at 6 K. (b) An empty-state STM image ($240\times 455\text{ \AA}^2$) with $V=1.5\text{ V}$ and $I=0.5\text{ nA}$ taken in the constant-current mode at 6 K. A three-dimensional island is seen in the center of the image. The straight out-of-phase boundary on the right of the image is also decorated by Ag adatoms. (c) An empty-state STM image ($260\times 260\text{ \AA}^2$) with $V=1.5\text{ V}$ and $I=0.4\text{ nA}$ taken in the constant-current mode at 6 K. Ag adsorbates are captured by the defect at the surface twin boundary between the IET+ and IET- domains.

IET structure. The high-symmetry $p31m$ of the HCT structure is thus reduced to $p3$ symmetry in the IET structure. Due to the asymmetry in the IET structure, there are two types of domains in the twin relation, defined as IET+ and IET-. A domain boundary seen in Fig. 1(c) is such a twin

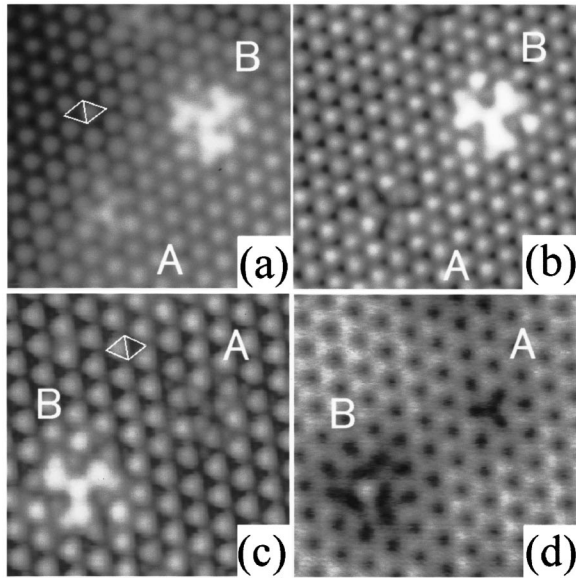


FIG. 2. Magnified STM images of the Ag adsorbates taken in the constant-current mode. The bias voltages, the tunneling currents, and the size of the images are (a) 1.3 V, 1.75 nA, and $77 \times 77 \text{ \AA}^2$; (b) 1.0 V, 1.0 nA, and $77 \times 77 \text{ \AA}^2$; (c) 0.5 V, 0.5 nA, and $65 \times 65 \text{ \AA}^2$; and (d) -1.0 V , 0.5 nA, and $65 \times 65 \text{ \AA}^2$, respectively. (a) and (b) were taken at the same area on the IET+ domain, while (c) and (d) were also taken at the same area on the IET- domain.

boundary, the right side of which is IET- and the left is IET+. The substrate in Figs. 2(a) and 2(b) is the IET+ domain, while that in Figs. 2(c) and 2(d) is the IET- domain; right halves in the unit cells in Figs. 2(a) and 2(b) are brighter, while they are darker in Fig. 2(c). These two types of domains cause the two types of orientation of the Ag stars and Ag propellers [compare them between Figs. 2(a) and 2(b) and in 2(c)]. Such difference is more clearly seen in Fig. 1(c). The orientations of Ag stars in this image are different between the upper right domain (IET-) and the lower left domain (IET+). The definition and detailed investigations on the IET structure are discussed elsewhere.^{12,13}

The bias dependence of the Ag stars and Ag propellers is also noted in Fig. 2. Figures 2(a) and 2(b) were taken at the same place with the bias voltages of 1.3 V and 1.0 V, respectively. The Ag-star pattern changes from the protrusionlike in Fig. 2(a) to the hollow patterns in Fig. 2(b). The center of the Ag star in Fig. 2(b) becomes dark, and the neighboring protrusions around the center become brighter. The pattern of the Ag propeller also changes with further changes in the bias voltage. Figures 2(c) and 2(d) were taken at the same area, but at the different area from the Figs. 2(a) and 2(b). Figure 2(c) is an empty-state STM image at a bias voltage of 0.5 V, while Fig. 2(d) is a filled-state image at the bias voltage of -1.0 V . Thus the bright patterns of the Ag propellers become darker and hollowed around at -1.0 V in Fig. 2(d).

These adsorbates are located sparsely and at roughly equal distances from each other on a terrace, as seen in Fig. 1(a). The step edge in the upper part in Fig. 1(a) and the domain boundary in Fig. 1(c) are decorated with such adsorbates, where more adsorbates are accommodated.

Those Ag adsorbates could not be observed when the $\sqrt{3} \times \sqrt{3}$ -Ag structure was prepared in a way such that the

amount of the Ag deposited at 500°C on the 7×7 surface was just 1 ML or less than 1 ML. Therefore, these Ag adsorbates originate from the excess Ag atoms ($1.7 \text{ ML} - 1.0 \text{ ML} = 0.7 \text{ ML}$ in this case) deposited during the formation of the $\sqrt{3} \times \sqrt{3}$ -Ag surface, though the amount of these adsorbates is on the order of 0.01 ML or less as discussed below.

The sample in Fig. 3 was prepared in the same way as in Figs. 1(a) and 1(b), but the temperature during the STM observation was at 62 K. Figures 3(a), 3(b), and 3(c) were successively taken; they took 55, 36, and 36 sec, respectively. The STM tip was scanned along a row from left to right, from the bottom row to the top in the images. Hazelike patterns can be seen, changing their positions in each figure. Some such bright patterns look like parts of the Ag propellers in the lower right of Fig. 3 near the step edge. Moreover the bias dependence of those hazelike patterns in the STM image is similar to that of the Ag adsorbates in Fig. 2. Thus it can be said that the hazelike patterns in Fig. 3 are Ag adsorbates migrating at a moderate speed to be observable.

The mobility of the Ag adsorbates increases with temperature. Considering that the Ag adsorbates are at rest at 6 K (Figs. 1 and 2), but moderately migrating at 62 K (Fig. 3), they must migrate with much higher speed at RT, forming the 2DAG phase. So the Ag adsorbates on the terrace in Fig. 1 correspond directly to the “frozen” 2DAG phase. The amount of those Ag adsorbates at 6 K approximately corresponds to the coverage of Ag atoms forming the 2DAG phase at 62 K, as discussed below.

B. Additional deposition

By depositing additional Ag atoms on the $\sqrt{3} \times \sqrt{3}$ -Ag substrate at 62 K¹⁵, it was observed that the Ag adatoms (Ag propellers) came together and made lattices of the $\sqrt{21} \times \sqrt{21}$ -(Ag+Ag) and the 6×6 -(Ag+Ag) superstructures. Though the Ag adsorbates have a moderate mobility at 62 K, as shown in Fig. 3, they become fixed with increasing population of the Ag adsorbates on the terraces of the $\sqrt{3} \times \sqrt{3}$ -Ag surface.

The sample in Fig. 4 was made in the following way: after preparing the $\sqrt{3} \times \sqrt{3}$ -Ag surface by depositing just 1 ML of Ag at 500°C , the sample was cooled down to 6 K, and then 0.09 ML of Ag was further deposited on it at 6 K. The Ag adsorbates are randomly located in Fig. 4(a), and some of the Ag propellers in a magnified image [Fig. 4(b)] do not have a complete shape with threefold symmetry as in Fig. 2. Ag atoms arriving on this very cold surface lose their kinetic energy and stop migrating so immediately that some of them cannot make the complete Ag propellers, and can not make lattices of the $\sqrt{21} \times \sqrt{21}$ or 6×6 superstructures.

What happens for these Ag adatoms when the substrate is annealed up to RT? After we obtained Fig. 4, 0.13 ML of Ag was further deposited at 6 K ($0.09 \text{ ML} + 0.13 \text{ ML} = 0.22 \text{ ML}$ in total). STM images with this coverage showed many more Ag stars and incomplete Ag propellers, which became difficult to distinguish from each other. The reason why we deposited further Ag atoms was to investigate the critical coverage of the 2DAG phase quantitatively, which will be discussed in Sec. III C in detail. While the sample is annealed from 6 K to RT, not only do the Ag adatoms rear-

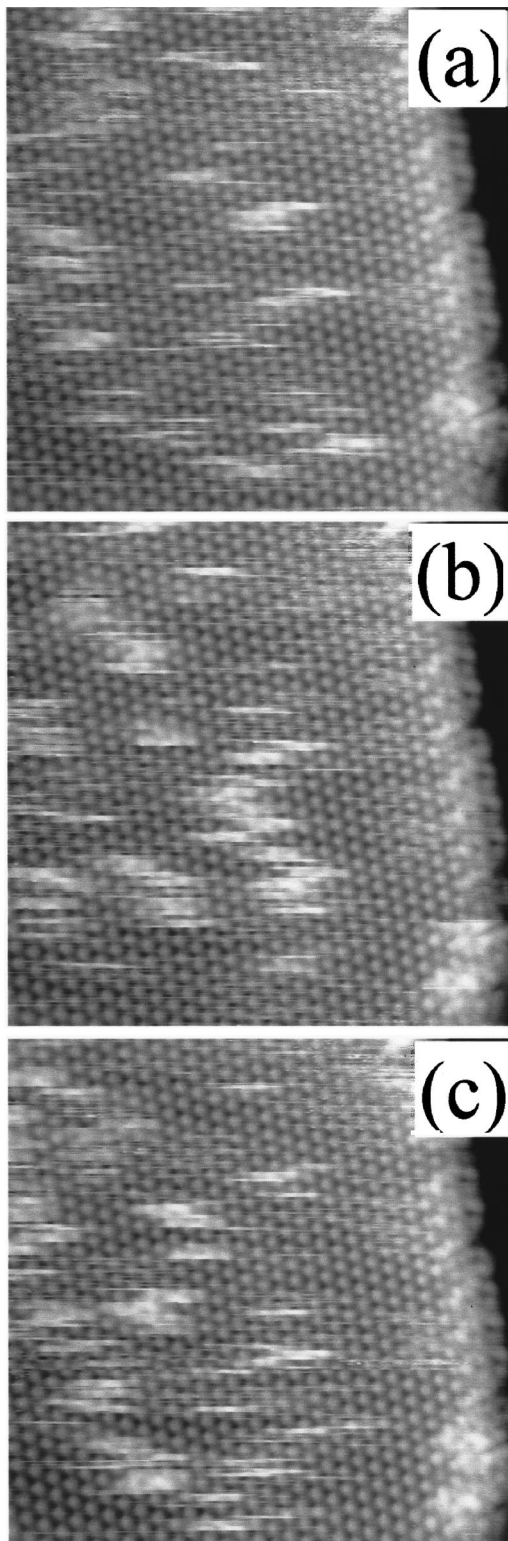


FIG. 3. Empty-state STM images ($190 \times 190 \text{ \AA}$) taken successively at 62 K, with $V=1.5 \text{ V}$ and $I=0.6 \text{ nA}$ in the constant-current mode. Images (b) and (c) were taken 65 and 111 s, respectively after image (a) was obtained.

range themselves, but the excess Ag adatoms form also 3D islands or are captured by defects, and there only remains a small amount of Ag adatoms as the 2DAG phase. In order to show the drastic decrease of the isolated Ag adsorbates (from 0.22 to 0.02 ML, as described in Sec. III C), we deposited further Ag atoms to an amount of 0.13 ML.

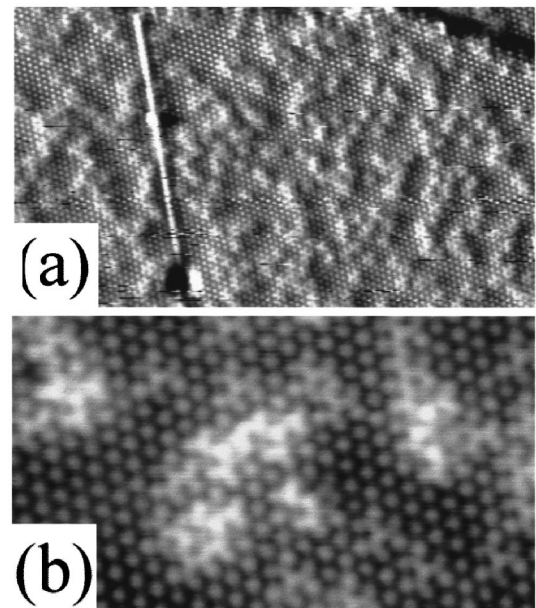


FIG. 4. (a) An empty-state STM image ($335 \times 580 \text{ \AA}^2$) with $V=1.5 \text{ V}$ and $I=0.2 \text{ nA}$ taken in the constant-height mode at 6 K. (b) A magnified image ($100 \times 175 \text{ \AA}^2$) of (a) with $V=1.4 \text{ V}$ and $I=0.5 \text{ nA}$ in the constant-current mode at 6 K.

After additional Ag deposition at 6 K, the sample was transferred to other places kept at RT in the vacuum chamber to warm up for about 3 h. Then it was again transferred back to the STM stage at 6 K and quenched. Figure 5 shows a surface prepared in this way. Since the annealing procedure gave enough thermal energy to the Ag adatoms for them to migrate and rearrange on the surface, most of the Ag stars in Fig. 4 coalesced into complete Ag propellers in Fig. 5. Also, the randomly dispersed Ag adsorbates in Fig. 4 changed their arrangement to be equidistant from each other, suggesting a repulsive interaction among the Ag propellers.

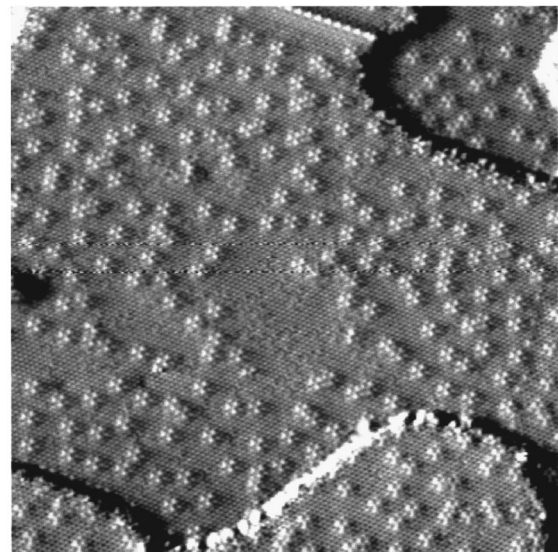


FIG. 5. An empty-state STM image ($715 \times 715 \text{ \AA}^2$) with $V=1.5 \text{ V}$ and $I=0.5 \text{ nA}$ in the constant-height mode at 6 K. Ag propellers are almost equally dispersed. A small number of Ag stars with hollowed patterns is also seen.

C. Density of 2DAG

The critical coverage (critical supersaturation) of the 2DAG phase $\Theta_C(T)$ is defined as the maximum coverage at which terraces can accommodate migrating isolated Ag adatoms without making 2D or 3D nuclei at temperature T . While cooling down to 6 K, the Ag adatoms lose their kinetic energy; some of them stay and come to rest on terraces, and others may come upon step edges and defects and be captured by them. Since the sample was quenched down to 6 K, the amount of migrating Ag adatoms captured by step edges and defects during cooling are thought to be small around the center of enough large terraces. Thus the amount of the Ag adatoms seen on terraces in Fig. 5 gives a measure of $\Theta_C(\text{RT})$ of the 2DAG phase or, at least, a lower limit of $\Theta_C(\text{RT})$. The amount of Ag adsorbates on the terraces in Fig. 5 was estimated in such a way that only the number of Ag propellers around the center on terraces was counted, and multiplied by 3, assuming that one Ag propeller consists of three Ag atoms. Since the number of Ag stars corresponding to single Ag adatoms is negligibly small in Fig. 5, the Ag stars were neglected. The amount of the Ag adsorbates thus estimated was about 0.02 ML. Thus, $\Theta_C(\text{RT})$ is approximated to be 0.02 ML, which is consistent with the value 0.03 ML previously obtained from the surface electrical conductance measurements.⁷ Even if one Ag propeller consisted of several atoms other than three atoms, it is certain that $\Theta_C(\text{RT})$ ranges from 0.01 to 0.1 ML.

The amount of Ag adatoms on terraces in Fig. 1(a) is about 0.003 ML, which gives the equilibrium density of the

2DAG. But this value is quite small compared to the amount of excess Ag atoms (0.7 ML) on top of the $\sqrt{3} \times \sqrt{3}$ -Ag substrate. Some of these decorate the step edges and domain boundaries as shown in Fig. 1, and others coalesce into 3D islands. Nevertheless, a very small amount of excess Ag atoms can still stay on terraces as in the 2DAG state. This means that the 2DAG phase is a thermodynamical equilibrium state with reservoirs like 3D islands and condensates at defects on the $\sqrt{3} \times \sqrt{3}$ -Ag surface.

IV. SUMMARY

We have directly shown the existence of 2DAG phase by low-temperature STM observations. Its frozen individual adatoms show characteristic bias-dependent starlike patterns. The density of the 2DAG estimated from the image of a quenched surface at 6 K was on the order of 0.01 ML, which is similar to that obtained from the previous surface electrical conductance measurements.⁷

ACKNOWLEDGMENTS

This work was supported in part by Grants-in-Aid from the Ministry of Education, Science, Culture, and Sports of Japan, especially through that for Creative Basic Research (No. 09NP1201) conducted by Professor K. Yagi of Tokyo Institute of Technology. We have also been supported by Core Research for Evolutional Science and Technology of the Japan Science and Technology Corporation conducted by Professor M. Aono of Osaka University and RIKEN.

*Author to whom correspondence should be addressed. Electronic address: shuji@surface.phys.s.u-tokyo.ac.jp

¹R. M. Tromp and M. Mankos, Phys. Rev. Lett. **81**, 1050 (1998).

²R. Kern, G. Lelay, and J. J. Metois, in *Current Topics in Materials Science*, edited by E. Kaldis (North-Holland, Amsterdam, 1979), Vol. 3, Chap. 3.

³S. Hasegawa, H. Daimon, and S. Ino, Surf. Sci. **186**, 138 (1987).

⁴H. Yasunaga and A. Natori, Surf. Sci. Rep. **15**, 205 (1992).

⁵L. S. O. Johansson, E. Landemark, C. J. Karlsson, and R. I. G. Uhrberg, Phys. Rev. Lett. **63**, 2092 (1989); **69**, 2451 (1992).

⁶S. Kono, K. Higashiyama, and T. Sagawa, Surf. Sci. **165**, 21 (1986).

⁷Y. Nakajima, G. Uchida, T. Nagao, and S. Hasegawa, Phys. Rev. B **54**, 14 134 (1996).

⁸Y. Nakajima, S. Takeda, T. Nagao, and S. Hasegawa, Phys. Rev. B **56**, 6782 (1997).

⁹A. Natori, M. Murayama, and H. Yasunaga, Surf. Sci. **357-358**, 47 (1996).

¹⁰T. Takahashi and S. Nakatani, Surf. Sci. **282**, 17 (1993), and references therein.

¹¹M. Katayama, R. S. Williams, M. Kato, E. Nomura, and M. Aono, Phys. Rev. Lett. **66**, 2762 (1991).

¹²H. Aizawa, M. Tsukada, N. Sato, and S. Hasegawa, Surf. Sci. Lett. **429**, L509 (1999).

¹³N. Sato, T. Nagao, and S. Hasegawa, Surf. Sci. **422**, 65 (1999).

¹⁴K. J. Wan, X. F. Lin, and J. Nogami, Phys. Rev. **45**, 9509 (1992).

¹⁵X. Tong, Y. Sugiura, T. Nagao, T. Takami, S. Takeda, S. Ino, and S. Hasegawa, Surf. Sci. **408**, 146 (1998).